Magnetic properties and the crystallization of amorphous $Fe_{75.4}B_{14.2}Si_{10.4}$

Hang Nam Ok, Kyung Seon Baek, and Chul Sung Kim
Department of Physics, Yonsei University, Seoul, Korea
(Received 18 June 1981)

The amorphous state of ferromagnetic $Fe_{75.4}B_{14.2}Si_{10.4}$ and its crystalline phases after crystallization have been studied by Mössbauer spectroscopy and magnetic-moment measurements. The average hyperfine field $H_{hf}(T)$ of the amorphous state shows a temperature dependence of $[H_{hf}(T)-H_{hf}(0)]/H_{hf}(0)=-0.30(T/T_c)^{3/2}-0.16(T/T_c)^{5/2}$ for $T/T_c<0.7$, indicative of spin-wave excitation. The quadrupole splitting just above T_c is 0.46 mm/s, whereas the average quadrupole shift below T_c is zero. The Curie and crystallization temperatures are determined to be $T_c=701$ K and $T_x=827$ K, respectively, for a heating rate of 11 K/min. The final products of crystallization are found to be Fe_2B and a Fe–18.1 at.% Si alloy. The saturation magnetic moment of the amorphous state extrapolated to 0 K is found to be $2.05\mu_B$/Fe atom. The magnetization of the amorphous phase decreases more rapidly with reduced temperature than those of crystalline ferromagnets. This kind of rapid decrease can be described in terms of either a distribution of exchange interactions in the amorphous phase or high metalloid contents.

I. INTRODUCTION

During recent years ferromagnetic amorphous alloys have appeared as a new class of magnetic materials. However, because these amorphous alloys are obtained by rapid quenching, they are not very stable, and various properties such as the magnetic hyperfine field[1] and the Curie temperature[2] are significantly changed by annealing treatments which do not cause crystallization. Furthermore, annealing at elevated temperatures inevitably causes crystallization due to which the excellent characteristics inherent in the amorphous structure are lost. In this paper we report on Mössbauer and magnetic measurements for amorphous $Fe_{75.4}B_{14.2}Si_{10.4}$ which has a very high crystallization temperature.

In Fe-based amorphous ferromagnets like the Fe-B system[3,4] or the $Fe_{78}B_{12}Si_{10}$ alloy,[5] α-Fe has been reported to precipitate during the crystallization processes. However, Ok and Morrish[1] found that a Fe-Si alloy instead of α-Fe is one of the crystalline products in a Fe-B-Si system like $Fe_{82}B_{12}Si_6$. The Mössbauer spectra of a large variety of amorphous alloys[3,4,6,7] are very similar and consist of structureless absorption lines that are broadened by distributions of magnetic hyperfine fields and quadrupole and isomer shifts. Various methods[6–8] have been employed to evaluate the hyperfine field distributions under the assumption of negligible broadening due to the distributions of quadrupole and isomer shifts. However, the broadening[9] due to quadrupole-shift distribution alone is found to be as large as 0.20 mm/s for $Fe_{82}B_{12}Si_6$, and thus any distribution analysis that does not include the quadrupole shift would be considerably limited in reliability.

The average magnetic hyperfine field measured at the Fe sites of a number of glassy ferromagnets[10] has been reported to decrease more rapidly with increasing temperature than that of crystalline Fe. This kind of rapid decrease has been described in terms of more spin-wave exictations[10] in the amorphous state than in the crystalline state, and in terms of a distribution of exchange interactions in amorphous ferromagnets.[3,11] However, an alternative interpretation may be possible in terms of a high metalloid content, because crystalline products also show similar behavior as will be shown later.

II. EXPERIMENTAL

The amorphous $Fe_{75.4}B_{14.2}Si_{10.4}$ was prepared by the roller quenching technique at the Research Institute for Iron, Steel and Other Metals, Tohoku University, Sendai, Japan. The samples were in the form of ribbons, 6 mm wide and 30 μm thick. A conventional constant acceleration Mössbauer spectrometer was used in conjunction with a 512-channel analyzer and a ^{57}Co source in a palladium host. The measurements above room temperature were made in a furnace with a temperature stability of 0.5 K. Those below room temperature were obtained in a cryostat with a stability of 0.2 K.

Magnetic moments were measured with a vibrating sample magnetometer calibrated with a pure nickel sample. In the same zone of the magnetometer a temperature range of 77–1050 K is available. All the measurements were performed by applying the external field in the plane of the ribbon in order to eliminate demagnetizing effects.

III. RESULTS AND DISCUSSION

A. Mössbauer spectra of the amorphous phase

Mössbauer spectra of the as-quenched amorphous $Fe_{75.4}B_{14.2}Si_{10.4}$ at temperatures below the Curie temperature T_c exhibit broadened six-line patterns as shown in Figs. 1 and 2. The broad lines are to be expected in view of the disordered atomic arrangements, in which the strength of the hyperfine interactions changes from site to site due to the structurally inequivalent Fe environments. This kind of broadened line may be analyzed in terms of the distribution[6–8] of magnetic hyperfine fields, assuming that broadening due to distributions of quadrupole splittings and isomer shifts are insignificant. However, the quadrupole splitting of amorphous $Fe_{75.4}B_{14.2}Si_{10.4}$ is as large as 0.46 mm/s at 711 K, and the line broadening[9] due to the distribution of quadrupole splittings is found to be

$$\frac{1}{\sqrt{5}}\frac{e^2qQ}{2}\left(1+\frac{1}{3}\eta^2\right)^{1/2}=\frac{1}{\sqrt{5}}(0.46)=0.21 \qquad (1)$$

expressed in units of mm/s. Other sources of broadening[9] come from the result of distributions of the isomer shift and the thickness effect of the absorber, which are estimated to be about 0.14 mm/s in view of the data on an iron foil 12.7 μm thick having a 0.23-mm/s linewidth and a quadrupole doublet linewidth of 0.37 mm/s above T_c for our amorphous sample. Thus, the combined broadening from distributions of quadrupole splitting and isomer shift including broadening due to the thickness effect amounts to about 0.35 mm/s below T_c, which may be large enough to make unreliable any analysis which does not include distributions of quadrupole and isomer shifts. Vincze[12] proposed a general method in which distributions of the quadrupole splitting and the isomer shift, in addition to the distribution of the magnetic hyperfine field, are included with an assumption of a linear relation between the distribution function of the magnetic hyperfine field and that of the quadrupole-isomer shift, $S(k)$, which is defined

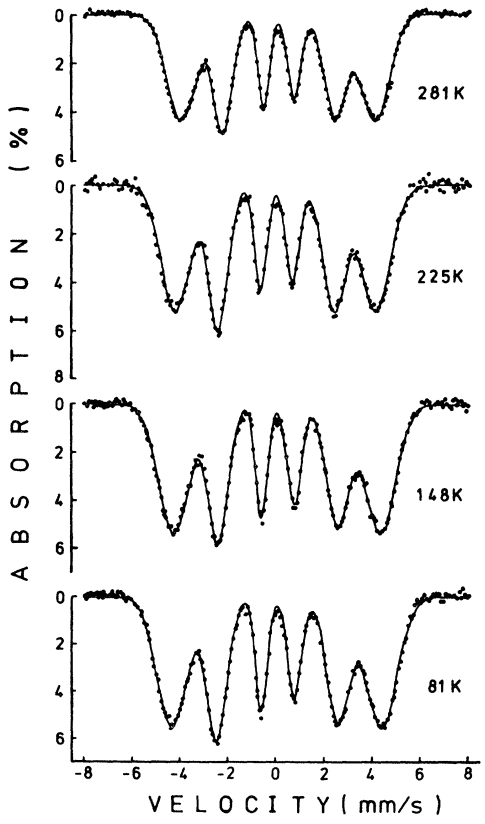

FIG. 1. Mössbauer spectra of $Fe_{75.4}B_{14.2}Si_{10.4}$ at low temperatures.

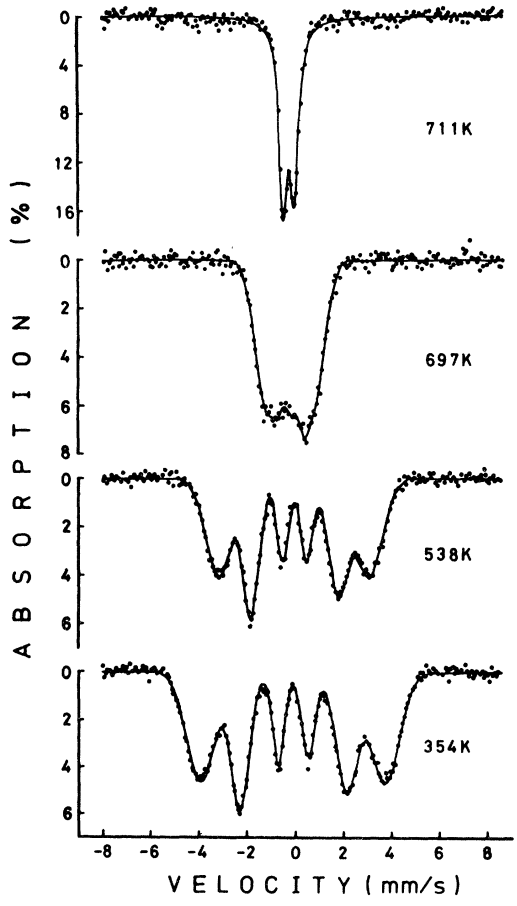

FIG. 2. Mössbauer spectra of $Fe_{75.4}B_{14.2}Si_{10.4}$ at high temperatures.

by

$$S(k)=S(0)+k(\delta\pm\tfrac{1}{2}\Delta E)\ , \qquad (2)$$

where the plus sign stands for lines 1 and 6 and the minus sign for lines 2, 3, 4, and 5 of a six-line pattern. $k=0,1,2,\ldots,z$. The basic idea of this method seems to be that each Fe nearest neighbor of a typical Fe atoms contributes an equal amount of isomer and quadrupole shift, namely, $\delta\pm\frac{1}{2}\Delta E$, where[9]

$$\Delta E=\tfrac{1}{4}e^2qQ(3\cos^2\theta-1+\eta\sin^2\theta\cos2\phi)\ . \qquad (3)$$

Here θ and ϕ are the angles, in polar coordinates, between the magnetic hyperfine-field vector and the principal axes of the electric-field-gradient tensor.

We applied this method to the Mössbauer spectrum taken at 281 K shown in Fig. 1, and calculated the distribution functions, $P(H_{hf})$ and $P(S)$, of the magnetic hyperfine field and the quadrupole-isomer shift, respectively. The results of these calculations are shown in Figs. 3 and 4. It is noted that the half-widths of the distribution function $P(S)$ are only 0.035 and 0.060 mm/s for lines 1 and 6 and 2–5, respectively, which are much smaller than the broadening due to the quadrupole shift alone as shown in Eq. (1). The reason for the discrepancy is not clear at this point. However, it is evident that each additional Fe nearest neighbor cannot contribute the same amount of quadrupole shift, ΔE, because ΔE depends on θ and ϕ according to Eq. (3).

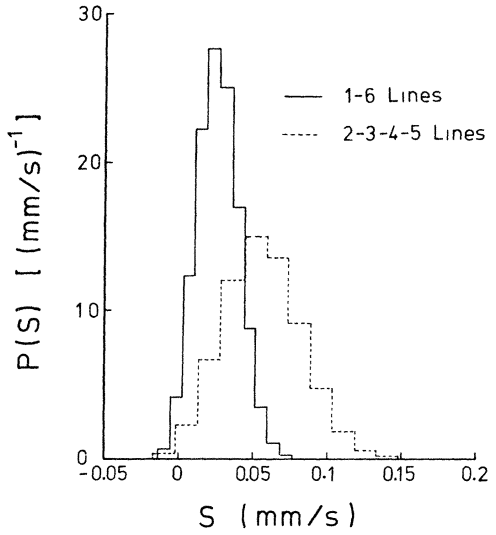

FIG. 4. Room-temperature distributions of the quadrupole-isomer shift of amorphous $Fe_{75.4}B_{14.2}Si_{10.4}$.

In the present analysis, no further attempt was made to get the distribution functions, and only average values were obtained by fitting six Gaussian lines to the Mössbauer spectra. The reason Gaussian line shapes were used instead of the usual Lorentzian line shapes was based on the result[7] that when the broadened absorption lines of amorphous solids were separated by an external magnetic field, the Gaussian line shapes gave better fits. In the present fit, lines symmetrically located in a six-line pattern are assumed to have the same areas. The average values of the magnetic hyperfine field and quadrupole splitting were obtained from least-squares fits, and are shown in Figs. 5 and 6.

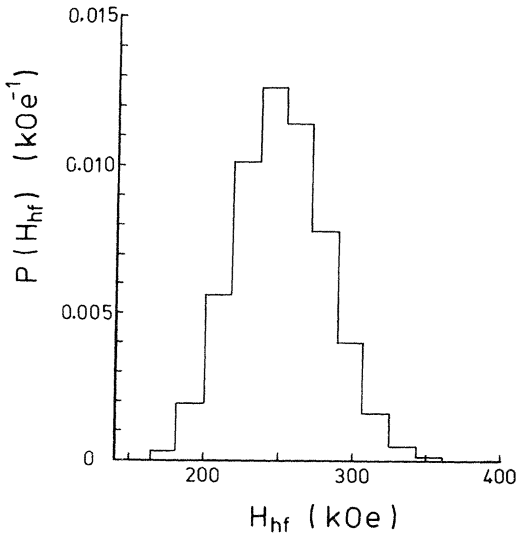

FIG. 3. The room-temperature hyperfine-field distribution of amorphous $Fe_{75.4}B_{14.2}Si_{10.4}$.

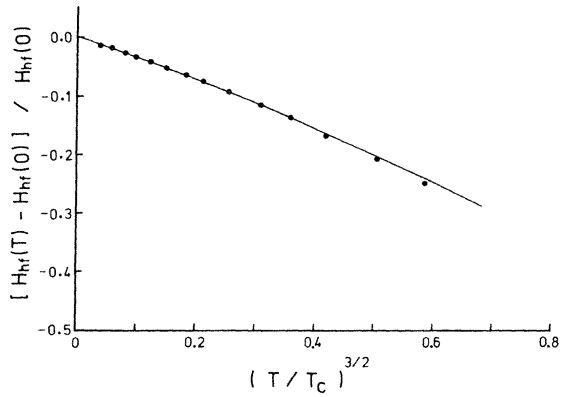

FIG. 5. Fractional change of the magnetic hyperfine field, H_{hf}, as a function of $(T/T_c)^{3/2}$.

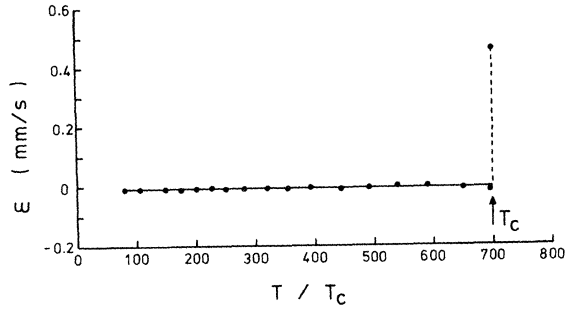

FIG. 6. Temperature dependence of the quadrupole shift ϵ.

B. Spin-wave excitations

Figure 5 shows the fractional change of the magnetic hyperfine field, $[H_{hf}(T)-H_{hf}(0)]/H_{hf}(0)$, as a function of T. For most amorphous ferromagnets[10] investigated so far, the magnetic hyperfine field decreases with increasing temperature according to

$$\frac{H_{hf}(T)-H_{hf}(0)}{H_{hf}(0)}=-B_{3/2}\left(\frac{T}{T_c}\right)^{3/2}-C_{5/2}\left(\frac{T}{T_c}\right)^{5/2} . \tag{4}$$

The temperature dependence of the leading term has its origin in the excitations of long-wavelength spin waves for which the detailed atomic arrangements are not important.[13] A least-squares fit of Eq. (4) to the magnetic hyperfing-field data gave $B_{3/2}=0.30\pm0.05$ and $C_{5/2}=0.16\pm0.05$. This value of $B_{3/2}$ for the amorphous ferromagnet $Fe_{75.4}B_{14.2}Si_{10.4}$ is much larger than those of crystalline ferromagnets[14] such as α-Fe and Ni; $B_{3/2}=0.12$ for Ni and $B_{3/2}=0.11$ for α-Fe. Apparently, more spin waves having long wavelengths are excited in amorphous ferromagnets than in crystalline ferromagnets.

C. Quadrupole splittings

Figure 6 shows the temperature dependence of the quadrupole splitting of $Fe_{75.4}B_{14.2}Si_{10.4}$. Above the Curie temperature, T_c, the quadrupole splitting is given by

$$\epsilon=\tfrac{1}{2}e^2qQ(1+\tfrac{1}{3}\eta^2)^{1/2} . \tag{5}$$

The value of ϵ was found to be 0.46 mm/s at 711 K, which is just above T_c. On the other hand, below T_c, ϵ has been calculated from the positions of the Mössbauer absorption lines from the expression

$$\epsilon=\tfrac{1}{2}(V_6-V_5+V_1-V_2) , \tag{6}$$

where V_i represents the position of the ith absorption line in mm/s.

When the quadrupole interaction is much weaker than the magnetic hyperfine interaction, the Mössbauer line shift from the quadrupole interaction can be described by ΔE of Eq. (3). On assuming that the maximum electric field gradient q and the asymmetry parameter η are independent of θ and ϕ, the average value of ΔE taken over all directions vanishes.[9] Since ϵ is related to ΔE by

$$\epsilon=\langle\Delta E\rangle , \tag{7}$$

the vanishing values of ϵ below T_c in Fig. 6 means that the magnetic hyperfine field is randomly oriented with respect to the principle axes of the electric field gradient.

D. Curie and crystallization temperatures

In order to determine the Curie temperature T_c and the cyrstallization temperature T_x, the velocity transducer of the Mössbauer spectrometer was set at zero velocity (zero velocity corresponds to the line position of the higher velocity component of the quadrupole doublet just above T_c) and counts were recorded for a fixed counting time of 14.5 s while the temperature was raised at a rate of 11 K/min from 300–863 K. The results are shown in Fig. 7.

At the disapparence of magnetic ordering, the count rate is expected to show a rapid decrease. From the graph the Curie temperature is determined to be 701 ± 2 K. As the temperature was further increased, the count rate increased slowly due to the second-order Doppler effect, and then increased suddenly at 827 K. This behavior results because the amorphous state is rapidly crystallizing and the Curie temperatures of the crystalline phases are higher than 827 K. After the amorphous $Fe_{75.4}B_{14.2}Si_{10.4}$ has reached the crystallization temperature $T_x=827$

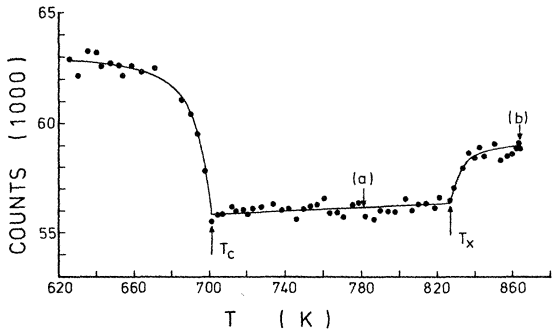

FIG. 7. Counts measured for 14.5 s at zero Doppler velocity as a function of temperature. The heating rate was 11 K/min.

±2 K, the amorphous state has been completely transformed into crystalline phases. In order to confirm that the sudden increase at T_x in Fig. 7 corresponds to crystallization, Mössbauer spectra of the sample were taken right before and after the second transition. Figure 8(a) is the Mössbauer spectrum taken at room temperature after cooling the sample down rapidly from 782 K indicated by (a) in Fig. 7. Figure 8(a) demonstrates that the sample is still amorphous. On the other hand, the Mössbauer spectrum, Fig. 8(b), taken at room temperature after cooling the sample down rapidly from 863 K, indicated by (b) in Fig. 7, shows that the sample is completely crystallized.

E. Structural relaxation

Table I shows magnetic hyperfine fields H_{hf} at room temperature, magnetic moments m at 82 K, and Curie temperatures T_c for the as-quenched $Fe_{75.4}B_{14.2}Si_{10.4}$ sample and the sample annealed at 782 K as indicated by (a) in Fig. 7. The Curie temperature of the annealed sample was determined from Fig. 9 by the counting method at a fixed velocity. From Table I, it is noted that the magnetic hyperfine field, magnetic moment, and Curie temperature increase upon annealing. One may suspect that possible partial crystallization[15] may be responsible for the increases. However, measurement of the magnetic moment at 82 K for the completely crystallized sample gave a smaller value of 176 emu/g, demonstrating that the main cause for the increases of H_{hf}, m, and T_c upon annealing is not partial crystallization. It is believed that the increases originate from strengthening of the long-range exchange interactions by the increase of atomic ordering during structural relaxation.[1]

F. Mössbauer spectra of the crystalline phases

Figures 8(b), 10, and 11 show Mössbauer spectra of the completely crystallized $Fe_{75.4}B_{14.2}Si_{10.4}$ taken at various temperatures. In contrast to Figs. 1 and 2 for the amorphous phase, the crystalline spectra consist of sharp absorption lines. Furthermore, the general pattern of the spectra changes twice as the temperature increases from liquid-nitrogen temperature to 1036 K; the first change takes place at 931 ±3 K from several sets of six-line patterns to a six-line pattern and a single line; the second one at 1020 ±5 K from a six-line plus a single-line pattern to a single line.

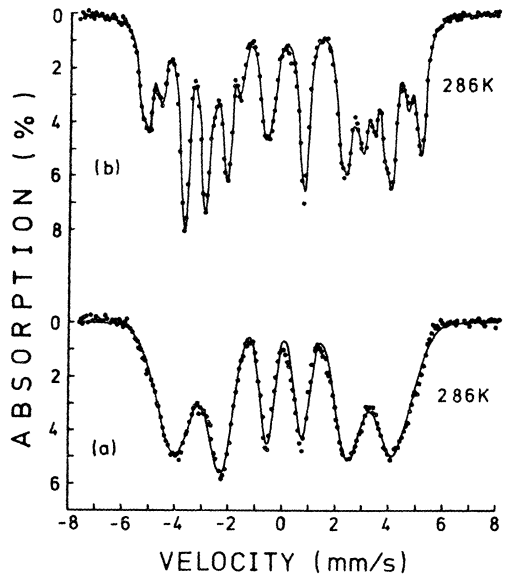

FIG. 8. Room-temperature Mössbauer spectra after annealing up to (a) 782 K and (b) 863 K at a rate of 11 K/min and cooling down rapidly to room temperature.

Least-squares fitting has been carried out using Lorentzian line shapes. In the present analysis, lines symmetrically located in a six-line pattern are assumed to have the same areas. Furthermore, the relative intensities of lines 1, 2, and 3 for each six-line pattern were assumed to be the same in a Mössbauer spectrum consisting of several sets of six-line patterns. All the Mössbauer spectra below 931 K can be satisfactorily fitted with six sets of six-line patterns; the results of the least-square fits are shown in Fig.

TABLE I. magnetic hyperfine fields H_{hf} at room temperature, magnetic moments m at 82 K, and Curie temperature T_c for the as-quencehed $Fe_{75.4}B_{14.2}Si_{10.4}$ sample and the sample annealed at 782 K as indicated by (a) in Fig. 7. The figures in parentheses are the probable errors.

Samples	H_{hf} (kOe)	m (emu/g)	T_c (K)
as-quenched	248 (1)	183 (1)	701 (2)
annealed	252 (1)	185 (1)	738 (2)

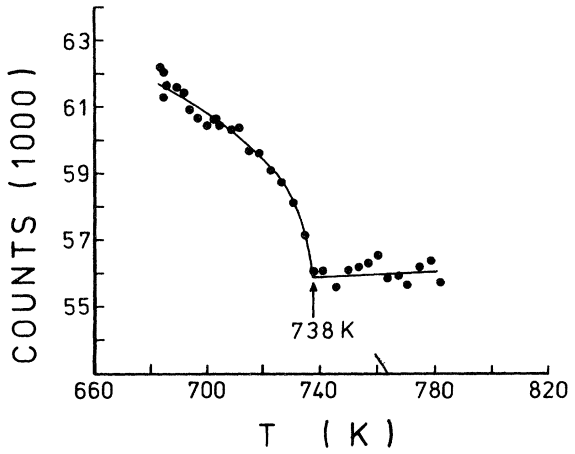

FIG. 9. Counts measured for 14.5 s at zero Doppler velocity as a function of temperature for the amorphous sample (a) in Fig. 8.

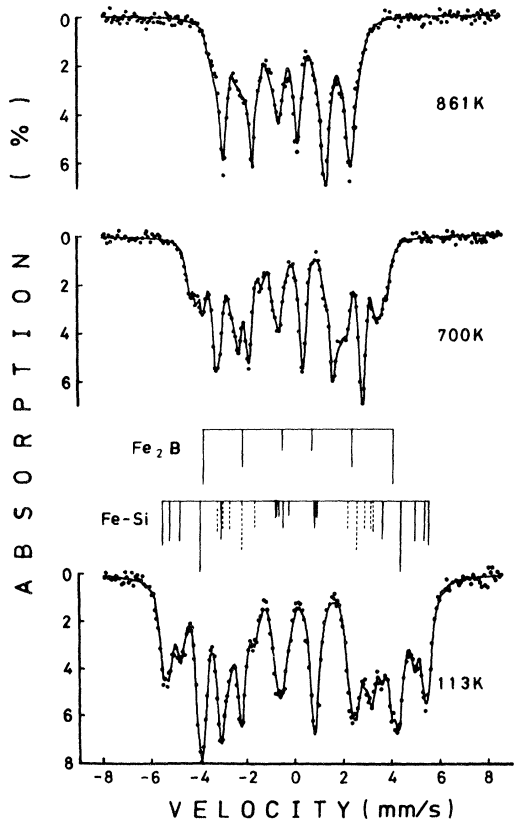

FIG. 10. Mössbauer spectra of the completely crystallized $Fe_{75.4}B_{14.2}Si_{10.4}$ at various temperatures.

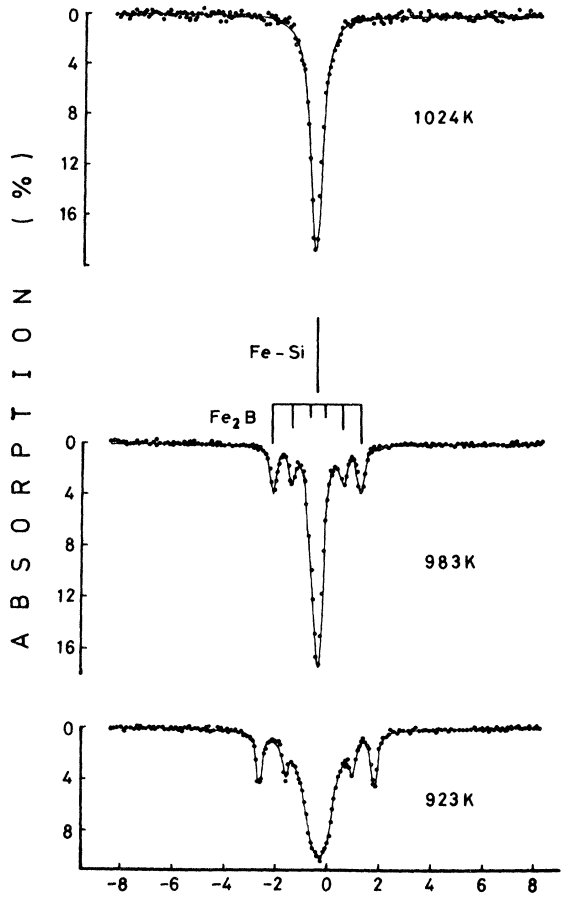

FIG. 11. Mössbauer spectra of the completely crystallized $Fe_{75.4}B_{14.2}Si_{10.4}$ at high temperatures.

12, from which it is evident that the completely crystallized $Fe_{75.4}B_{14.2}Si_{10.4}$ consists of two phases; one phase has a magnetic hyperfine field of 237 kOe at room temperature and a Curie temperature of 1020 ± 5 K. From a comparison with the Curie temperature of 1015 ± 5 K and the magnetic hyperfine field of 237 kOe at room temperature for Fe_2B,[16] this phase can be identified with Fe_2B. X-ray studies also confirm the existence of tetragonal Fe_2B with lattice constants of $a_0 = 5.109$ A and $c_0 = 4.249$ A, which are in good agreement with those[17] reported. The other phase has a lower Curie temperature of 931 K, and consists of five different magnetic sites whose magnetic hyperfine fields at room temperature are shown in Table II. X-ray-diffraction patterns for the crystallized $Fe_{75.4}B_{14.2}Si_{10.4}$ show very strong bcc lines in addition to the tetragonal Fe_2B lines. Since the solubility of boron in the bcc iron lattice is extremely small (only 0.0002 wt.% at 983 K),[18] and Fe-Si alloys are known to have the bcc structure for low Si concentrations,[19] one may assume that the crystallization of

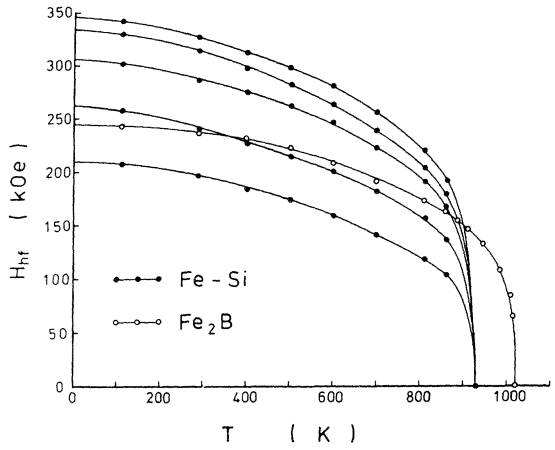

FIG. 12. Temperature dependence of the hyperfine field of the crystalline phases after crystallization.

$Fe_{75.4}B_{14.2}Si_{10.4}$ proceeds according to the following equation

$$Fe_{75.4}B_{14.2}Si_{10.4} \rightarrow 14.2Fe_2B + Fe_{47}Si_{10.4} \ . \quad (8)$$

In order to prove this assumption, a sample of $Fe_{47}Si_{10.4}$, or Fe–18.1 at.% Si, was prepared by grinding together appropriate proportions of Fe and Si powders of 99.995% purities, pressing the resulting mixture into a pellet under a pressure of 5300 kg/cm^2 and firing in an evacuated quartz tube at 1050 °C for 5 h. Mössbauer spectra of this sample were taken at room temperature and at various temperatures near the Curie temperature. The room-temperature spectrum can be satisfactorily fitted with five sets of six-line patterns, and the results of the least-square fits are shown in Table II. An x-ray-diffraction pattern was also taken for this sample, and it showed only bcc lines. From comparison of the data in Table II, one can conclude that the second phase of the crystallized $Fe_{75.4}B_{14.2}Si_{10.4}$ is $Fe_{47}Si_{10.4}$, thus proving Eq. (8).

G. Temperature dependence of $H_{hf}(T)$

Figure 13 shows the temperature dependence of the magnetic hyperfine field in reduced units for the amorphous $Fe_{75.4}B_{14.2}Si_{10.4}$ and crystalline α-Fe.[20] It is clearly seen that $H_{hf}(T)/H_{hf}(0)$ decreases with T/T_c more rapidly in the amorphous $Fe_{75.4}B_{14.2}Si_{10.4}$ than in crystalline Fe. This "flattening" of $H_{hf}(T)/H_{hf}(0)$ or $M(T)/M(0)$ has been observed in many other amorphous ferromagnets,[21,22] and is often described by a model that considers the random distribution of exchange constants $J(r_{ij})$ in the mean-field approximation developed by Handrich.[11] He shows that the reduced magnetization can be written

$$\sigma(\tau) = M(T)/M(0) = \tfrac{1}{2}B_S[(1+\delta)x] + \tfrac{1}{2}B_S[(1-\delta)x] \ , \quad (9)$$

where B_S is the Brillouin function, $x = 3S\sigma/(S+1)$, $\tau = T/T_c$, and $\delta = \langle \Delta J_{12} \Delta J_{13} \rangle^{1/2} / \langle J_{12} \rangle$. Here δ is a measure of the fluctuations in the exchange interaction, and lies between 0 and 1. The curve for $\delta = 0$ corresponds to the crystalline case. The calculated curves are progressively lower for increasing values of δ, and give generally poor fits to the experimental values, suggesting that the model is inadequate. Actually, the difference between the reduced magnetic hyperfine fields of the amorphous and crystalline $Fe_{75.4}B_{14.2}Si_{10.4}$ alloys is substantially smaller and the

TABLE II. Magnetic hyperfine fields H_{hf} at room temperature, Curie temperature T_c, and lattice parameter a_0 for the bcc phase of the crystallized $Fe_{75.4}B_{14.2}Si_{10.4}$ and the Fe–18.1 at.% Si alloy. The figures in parentheses are the probable errors.

Crystals	H_{hf} (kOe)	T_c (K)	a_0 (A)
bcc phase of the crystallized $Fe_{75.4}B_{14.2}Si_{10.4}$	326 (3) 312 (3) 285 (3) 240 (3) 196 (3)	931 (3)	2.836 (2)
Fe–18.1 at.% Si alloy	325 (3) 306 (3) 284 (3) 244 (3) 192 (3)	931 (3)	2.836 (2)

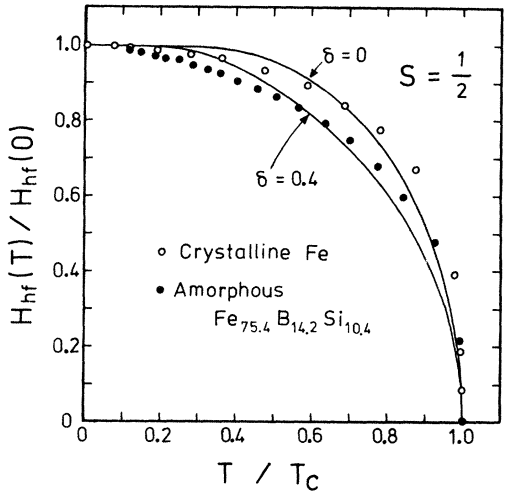

FIG. 13. Reduced hyperfine field vs reduced temperature of $Fe_{75.4}B_{14.2}Si_{10.4}$ and Fe metal. The solid curves are results obtained from Eq. (9).

reduced hyperfine field in both states decreases much faster with T/T_c than in metallic iron as shown in Fig. 14. These results suggest an alternative interpretation that structural disorder has a minor effect on the shape of $\sigma(\tau)$ and that high metalloid content is responsible for the fast decrease of $H_{hf}(T)/H_{hf}(0)$ in these materials. Furthermore, this decrease of $\sigma(\tau)$ seems to depend on the kind of metalloid atoms; Si atoms are more effective in reducting the magnetic hyperfine field than B atoms, as can be seen in Fig. 14.

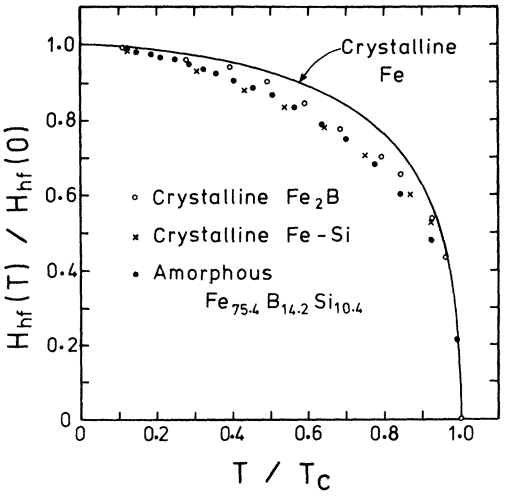

FIG. 14. Reduced hyperfine field vs reduced temperature of amorphous $Fe_{75.4}B_{14.2}Si_{10.4}$ and the crystalline phases after crystallization.

H. Magnetic moments

The magnetic moment of the amorphous $Fe_{75.4}B_{14.2}Si_{10.4}$ has been measured at $H=8$ kOe at various temperatures from liquid-nitrogen temperature to the Curie temperature of the sample. The results are shown in Fig. 15 in reduced units along with the magnetic hyperfine fields obtained from the Mössbauer spectra. From Fig. 15, it is evident that the magnetic moment is proportional to the magnetic hyperfine field in the amorphous $Fe_{75.4}B_{14.2}Si_{10.4}$. The saturation magnetic moment at 0 K extrapolated using Eq. (4) is 185 emu/g or $2.05\mu_B$/Fe atom. This value is smaller than the $2.3\mu_B$ of "pure" amorphous Fe (Ref. 23) or the $2.22\mu_B$ of bcc Fe.[24] This kind of reduction in the magnetic moment of transition-metal atoms in metallic glasses[25] is generally believed to arise from electron transfer from the metalloid atoms to the transition-metal atoms. Figure 16 shows how the magnetization changes during heating and cooling processes, according to the magnetic and crystallographic phase transitions of the sample. The room-temperature saturation value of the magnetization of the as-quenched amorphous $Fe_{75.4}B_{14.2}Si_{10.4}$ is found to be 164 ±1 emu/g. As the temperature increases, magnetization decreases rapidly near 700 K. The ferromagnetic Curie temperature T_c, determined under a residual field, is 705 ±5 K, which is in good agreement with 701 ±2 K measured with the Mössbauer counting technique. This value is higher than those for $Fe_{80}B_{20}$($T_c=685$ K)[3], for $Fe_{82}B_{12}Si_6$($T_c=658$ K),[9] for $Fe_{40}Ni_{40}P_{14}B_6$($T_c=537$ K),[10] and for $Fe_{75}P_{15}C_{10}$($T_c=619$ K).[10] It is evident, then, that $Fe_{75.4}B_{14.2}Si_{10.4}$ has a smaller temperature dependence for magnetic properties around room temperature, an advantage for magnetic device applications.

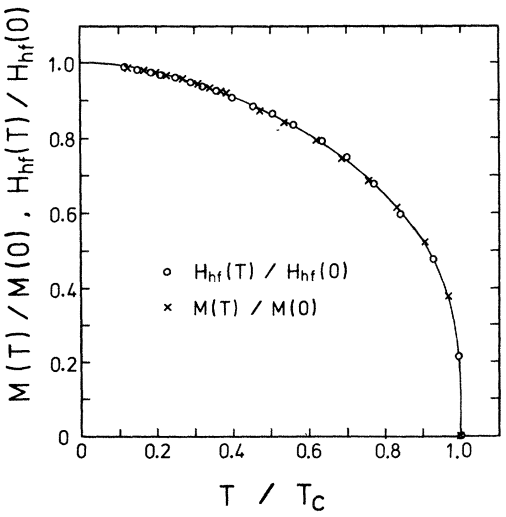

FIG. 15. Reduced magnetization and hyperfine field vs reduced temperature of the amorphous $Fe_{75.4}B_{14.2}Si_{10.4}$.

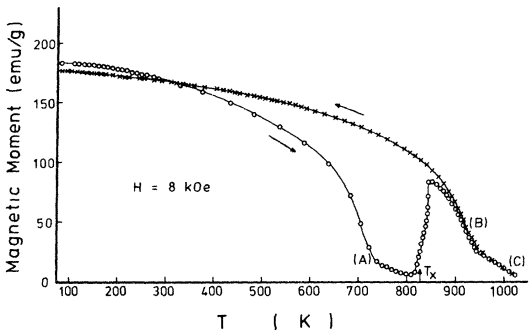

FIG. 16. Temperature dependence of magnetization for $Fe_{75.4}B_{14.2}Si_{10.4}$. The arrows indicate the temperature cycle.

In order to determine the crystallization temperature of the amorphous sample, the temperature was increased at a high heating rate of 11 K/min from 750 K. As shown in Fig. 16, a sudden increase of magnetization due to crystallization has been observed at $T_x = 827 \pm 3$ K, which is the same value as that obtained with the Mössbauer technique. This value of T_x is one of the highest so far reported; for example, $T_x = 700$ K for $Fe_{40}Ni_{40}P_{14}B_6$ (Metglas® 2826)[22], $T_x = 715$ K for $Fe_{80}B_{20}$[3], and $T_x = 780$ K for $Fe_{82}B_{12}Si_6$ (Metglas® 2605 S)[9]. The high value of $T_x = 827$ K for $Fe_{75.4}B_{14.2}Si_{10.4}$ indicates the superior structural stability of this material. After completion of crystallization, the magnetization decreases rapidly again above 900 K as indicated by (B) in Fig. 16, which corresponds to $T_c = 931$ K of the Fe–18.1 at.% Si alloy, one of the crystalline products of $Fe_{75.4}B_{14.2}Si_{10.4}$. Magnetization does not vanish until the temperature rises above 1000 K as indicated by (C) in Fig. 16, which corresponds to $T_c = 1020$ K of Fe_2B, the other of the crystalline products.

IV. CONCLUSIONS

The amorphous state of the ferromagnetic $Fe_{75.4}B_{14.2}Si_{10.4}$, and the crystalline phases after crystallization have been studied by ^{57}Fe Mössbauer spectroscopy and magnetic-moment measurements from liquid-nitrogen temperature to 1036 K.

From broadened Mössbauer patterns in the amorphous state, a hyperfine-field distribution $P(H_{hf})$ has been determined along with a distribution function $P(S)$ of the quadrupole-isomer shift under the assumption of a linear relation between $P(H_{hf})$ and $P(S)$. The half-widths of the $P(S)$ functions are found to be substantially smaller than the line-broadening of 0.21 mm/s calculated under the assumption of random orientation of the magnetic hyperfine field with respect to the electric field gradient. This assumption of random orientation of the magnetic hyperfine field is supported by the observation of a vanishing average quadrupole shift below T_c and a nonzero quadrupole splitting of 0.46 mm/s above T_c.

At low temperatures the values of the magnetic hyperfine field $H_{hf}(T)$ show a $T^{3/2}$ dependence that is related to the preferential excitation of long-wavelength spin waves. The $T^{3/2}$ coefficient is about three times as large as those of crystalline Fe or Ni. Consequently, the reduced hyperfine field $H_{hf}(T)/H_{hf}(0)$ or equivalently the reduced magnetization $M(T)/M(0)$ of the amorphous phase decreases more rapidly with reduced temperature T/T_c than those of crystalline ferromagnets. This kind of rapid decrease can be described in terms of either a distribution of exchange interactions in the amorphous phase or high metalloid contents.

Before the onset of crystallization, the magnetic hyperfine field, magnetic moment, and Curie temperature of the amorphous phase have been observed to increase. These increases are believed to arise from strengthening of the long-range exchange interactions by the increase of atomic ordering during structural relaxation.[1]

The Curie and crystallization temperatures are determined to be $T_c = 701$ K and $T_x = 827$ K, respectively, at a heating rate of 11 K/min. The saturation magnetic moment of the as-quenched amorphous state extrapolated to 0 K is found to be $2.05\mu_B$/Fe atom, suggesting electron transfer from the metalloid atoms to the d band of the Fe atoms. Examination of the Mössbauer spectra and x-ray diffraction patterns taken for the crystallized $Fe_{75.4}B_{14.2}Si_{10.4}$ and Fe–18.1 at.% Si alloy shows that the crystalline products are Fe_2B and a Fe–18.1 at.% Si alloy.

ACKNOWLEDGMENT

Financial support for this research was obtained through a grant from the Ministry of Education, the Republic of Korea.

[1]Hang Nam Ok and A. H. Morrish, Phys. Rev. B 22, 3471 (1980).
[2]H. H. Liebermann, C. D. Graham Jr., and P. J. Flanders, IEEE Trans. Magn. 13, 1541 (1977).
[3]C. C. Chien, Phys. Rev. B 18, 1003 (1978).
[4]T. Kemeny, I. Vincze, and B. Fogarassy, Phys. Rev. B 20, 476 (1979).
[5]T. Masumoto, H. Kimura, A. Inoue, and Y. Waseda,

Mater. Sci. Eng. 23, 141 (1976).
[6]T. E. Sharon and C. C. Tsuei, Phys. Rev. B 5, 1047 (1972).
[7]P. J. Schurer and A. H. Morrish, Solid State Commun. 28, 819 (1978).
[8]B. Window, J. Phys. E 4, 401 (1971).
[9]Hang Nam Ok and A. H. Morrish, Phys. Rev. B 22, 4215 (1980).
[10]C. L. Chien and R. Hasegawa, Phys. Rev. B 16, 2115 (1977).
[11]K. Handrich, Phys. Status Solidi 32, K55 (1969).
[12]I. Vincze, Solid State Commun. 25, 689 (1978).
[13]C. Herring and C. Kittel, Phys. Rev. 81, 869 (1951).
[14]B. E. Argyle, S. H. Charap, and E. W. Pugh, Phys. Rev. 132, 2051 (1963).
[15]S. Hatta, T. Egami, and C. D. Graham, Jr., Appl. Phys. Lett. 34, 113 (1979).
[16]L. Takács, M. C. Cadeville, and I. Vincze, J. Phys. F 5, 800 (1975).
[17]R. W. G. Wyckoff, *Crystal Structures* (Interscience, New York, 1963), Vol. 1, p. 361.
[18]C. C. McBride, J. W. Spretnak, and R. Speiser, Trans. Am. Soc. Met. 46, 499 (1954).
[19]H. Z. Warlimont, Z. Metallkd. 59, 595 (1968).
[20]R. S. Preston, S. S. Hanna, and J. Herberle, Phys. Rev. 128, 2207 (1962).
[21]C. C. Tsuei and H. Lilienthal, Phys. Rev. B 13, 4899 (1976).
[22]C. L. Chien and R. Hasegawa, Phys. Rev. B 16, 3024 (1977).
[23]J. Durand, IEEE Trans. Magn. 12, 945 (1976).
[24]R. S. Tebble and D. J. Craik, *Magnetic Materials* (Wiley-Interscience, New York, 1969), p. 51.
[25]J. J. Beck, F. E. Luborsky, and J. L. Walter, IEEE Trans. Magn. 13, 988 (1977); R. C. O'handley and D. S. Boudreaux, Phys. Status Solidi A 45, 607 (1978).